J|A|C|S
ARTICLES

Published on Web 08/13/2009

Single Gold Nanoparticles Counter: An Ultrasensitive Detection Platform for One-Step Homogeneous Immunoassays and DNA Hybridization Assays

Chao Xie, Fagong Xu, Xiangyi Huang, Chaoqing Dong, and Jicun Ren*

College of Chemistry and Chemical Engineering, State Key Laboratory of Metal Matrix Composites, Shanghai Jiaotong University, 800 Dongchuan Road, Shanghai 200240, P.R. China

Received May 19, 2009; E-mail: jicunren@sjtu.edu.cn

Abstract: In this paper, we present for the first time a single gold nanoparticle counter (SGNPC) in solution based on the photon bursting in a highly focused laser beam (less than 1 fL) due to the plasmon resonance scattering and Brownian motion of gold nanoparticles (GNPs). The photon burst intensity of single 36 nm GNPs is several tens to hundreds times stronger than that of quantum dots (QDs) and organic dyes. The relationship between the photon burst counts and GNPs concentration shows an excellent linearity. The linear range is over 4 orders of magnitude, and the detection limit of GNPs (36 nm) is 17 fM. On the basis of this single nanoparticle technique, we developed an ultrasensitive and highly selective detection platform for homogeneous immunoassay and DNA hybridization assays using GNPs as probes, which were 2−5 orders of magnitude more sensitive than current homogeneous methods. We used this technology to construct homogeneous sandwich immunoassays for cancer biomarkers, such as carcinoembryonic antigen (CEA) and alpha fetal protein (AFP), and aptamer recognition for thrombin. The detection limits are 130 fM for CEA, 714 fM for AFP and 2.72 pM for thrombin. Our method was successfully applied for direct determination of CEA, AFP and thrombin levels in sera from healthy subjects and cancer patients. In homogeneous DNA hybridization detection, we chose methylenetetrahydrofolate reductase (MTHFR) gene as a target. This assay successfully distinguished DNA sequences with single base mismatches, and the detection limits for the target were at 1 fM level.

Introduction

Currently, immunoassay and nucleic acid hybridization are the most widely used bioassays, and they play very important roles in clinical diagnosis, food and environmental analyses, and biological and biomedicine studies.[1−7] The conventional heterogeneous immunoassays and nucleic acids hybridization assays have some advantages such as high specificity, low background and high throughput. However, conventional assay formats involve antibodies or oligonucleotides immobilization, incubation and washing cycles, and thus they are considered to be labor-intensive and time-consuming.[8−11] Generally, homogeneous assays are attractive detection formats because they are amenable to automation, reduce the risk of contamination and eliminate time-consuming washing steps/sample handling. The key technique in homogeneous bioassays is how to quantitatively and sensitively distinguish properties of antigen−antibody complexes and hybridization products in the complicated reaction solution. To date, several analytical methods have been used in homogeneous immunoassays, such as fluorescence polarization[12,13] and fluorescence resonance energy transfer.[14−17] However, the sensitivity of these homogeneous detection methods is unsatisfactory.

Gold nanoparticles (GNPs) are very attractive labels due to their extremely strong absorption and light scattering in the plasmon resonance wavelength regions and certain fluorescence properties.[18−21] Compared to current fluorescent probes (organic dyes and quantum dots), GNPs have special physical and

(1) Loos, R. J. F.; et al. *Nat. Genet.* **2008**, *40*, 768−775.
(2) Bailey, R. C.; Kwong, G. A.; Radu, C. G.; Witte, O. N.; Heath, J. R. *J. Am. Chem. Soc.* **2007**, *129*, 1959–1967.
(3) Hayden, E. C. *Nature* **2008**, *456*, 850–850.
(4) Ke, Y. G.; Lindsay, S.; Chang, Y.; Liu, Y.; Yan, H. *Science* **2008**, *319*, 180–183.
(5) Lee, C.; Iafrate, A. J.; Brothman, A. R. *Nat. Genet.* **2007**, *39*, S48−S54.
(6) Porter, M. D.; Lipert, R. J.; Siperko, L. M.; Wang, G.; Narayanana, R. *Chem. Soc. Rev.* **2008**, *37*, 1001–1011.
(7) Freeman, R. G.; Hommer, M. B.; Grabar, K. C.; Jackson, M. A.; Natan, M. J. *J. Phys. Chem.* **1996**, *100*, 718–724.
(8) Narayanan, R.; Lipert, R. J.; Porter, M. D. *Anal. Chem.* **2008**, *80*, 2265–2271.
(9) Sharlow, E. R.; Leimgruber, S.; Yellow-Duke, A.; Barrett, R.; Wang, Q. J.; Lazo, J. S. *Nat. Protoc.* **2008**, *3*, 1350–1363.
(10) Heyduk, E.; Dummit, B.; Chang, Y. H.; Heyduk, T. *Anal. Chem.* **2008**, *80*, 5152–5159.
(11) Ramirez, D. C.; Gomez-Mejiba, S. E.; Mason, R. P. *Nat. Protoc.* **2007**, *2*, 512–522.
(12) Tachi, T.; Kaji, N.; Tokeshi, M.; Baba, Y. *Lab Chip* **2009**, *9*, 966–971.
(13) Cruz-Aguado, J. A.; Penner, G. *Anal. Chem.* **2008**, *80*, 8853–8855.
(14) Yang, R. H.; Jin, J. Y.; Chen, Y.; Shao, N.; Kang, H. Z.; Xiao, Z.; Tang, Z. W.; Wu, Y. R.; Zhu, Z.; Tan, W. H. *J. Am. Chem. Soc.* **2008**, *130*, 8351–8358.
(15) Lopez-Crapez, E.; Malinge, J. M.; Gatchitch, F.; Casano, L.; Langlois, T.; Pugniere, M.; Roquet, F.; Mathis, G.; Bazin, H. *Anal. Biochem.* **2008**, *383*, 301–306.
(16) Liu, L.; Shao, M.; Dong, X.; Yu, X.; Liu, Z.; He, Z.; Wang, Q. *Anal. Chem.* **2008**, *80*, 7735–7741.
(17) Kokko, T.; Liljenback, T.; Peltola, M. T.; Kokko, L.; Soukka, T. *Anal. Chem.* **2008**, *80*, 9763–9768.
(18) Zhang, K.; Yang, H. *J. Phys. Chem. B* **2005**, *109*, 21930–21937.

chemical properties, such as no photobleaching and blinking, ease of synthesis, simplicity of conjugation chemistry and excellent biocompatibility. Due to their excellent features, GNPs as probes have been used in bioassays,[22−27] single particle tracking,[28−30] and cell imaging.[31−35] So far, colorimetric and scattering detections including dynamic light scattering are mostly used in GNPs-based heterogeneous immunoassays and DNA hybridization with high sensitivity.[36−44] However, in homogeneous formats, the absorption and scattering signals of the bulk solution do not change significantly before and after the reaction, and current colorimetric and scattering techniques are difficult to directly determine the low concentration of samples in clinical diagnosis.

Herein, we present a novel method for detection of GNPs in solution at single particle level, which is called as a single GNPs counter (SGNPC). Its principle is based on the photon burst counting in a small detection volume (less than 1 fL) due to strong resonance scattering and Brownian motion of single GNPs. The relationship between the photon burst counts and the GNPs concentration showed an excellent linearity. On the basis of this technique, we developed an ultrasensitive and highly selective detection platform for homogeneous immunoassays and DNA hybridization assays, which were 2−5 orders of magnitude more sensitive than the current homogeneous methods. In homogeneous assays, we used a sandwich strategy and conjugated two probes (antibodies, aptamers and oligonucleotides) with GNPs respectively. When two GNPs−probe conjugates are mixed in a sample containing targets (such as antigens and DNA targets) the binding of targets will cause GNPs to form dimers (or oligomers). We reasoned that the number of GNPs decreased with an increase of targets in solution, and SGNPC detected the change in the number of GNPs according to the photon burst counts. We used this technology to construct homogeneous immunoassays for cancer biomarkers, such as carcinoembryonic antigen (CEA) and alpha fetal protein (AFP), and aptamer recognition for thrombin. The detection limits are 130 fM for CEA, 714 fM for AFP and 2.72 pM for thrombin. Our method was successfully applied for direct determination of CEA and AFP levels in sera and thrombin level in plasma from healthy subjects and cancer patients. Our results were in good agreement with ELISA assays and capillary electrophoresis data. In homogeneous DNA hybridization detection, we chose methylenetetrahydrofolate reductase (MTHFR) gene as a target. The detection limits are at 1 fM level, and the linear ranges are close to 2 orders of magnitude. This assay unambiguously distinguished DNA sequences with single base mismatches.

Experimental Section

Chemicals and Materials. Mouse antihuman monoclonal 1C11 antibody to carcinoembryonic antigen (anti-CEA-1), mouse antihuman monoclonal 1C7 antibody to CEA (anti-CEA-2) and CEA antigen protein were purchased from Abcam plc. (Cambridge, U.K.). Mouse antihuman monoclonal alpha fetal protein antibodies (anti-AFP-1 and anti-AFP-2), AFP antigen protein, ELISA kits for human CEA and AFP were purchased from Beijing North Institute of Biological Technology (Beijing, China). Thrombin and bovine serum albumin (BSA) were obtained from Sigma-Aldrich Chemical Co. (Milwaukee, U.S.A.). The aptamers and oligonucleotides were purchased from Sangon Biological Engineering Technology and Services Co., Ltd. (Shanghai, China). Hydrogen tetrachloroaurate (III) hydrate ($HAuCl_4$) was purchased from Yiyang Chemical Co., Ltd. (Shanghai, China). CdSe quantum dots (Qdot 655, emission wavelength of 655 nm) and Alexa 647 were purchased from Invitrogen Co. (California, U.S.A.). Ultrapure water (18.2 MΩ) was obtained from the Millipore Simplicity System (Millipore, Bedford, MA, U.S.A.). All other reagents were obtained from Sigma-Aldrich Chemical Co. (Milwaukee, U.S.A.).

Five human sera from healthy subjects (samples 1−5), one pregnant woman serum (sample 6) and four human plasma were obtained from volunteers in our laboratory. Three cancer patient sera (samples 7−9) were provided by Shanghai Jiaotong University Affiliated Shanghai First People's Hospital. Serum samples were clotted for 30 min at room temperature and centrifuged (Beckman Coulter, U.S.A.) at 2500 rpm for 10 min, and the serum samples were stored at 4 °C for further use. Human plasma samples were obtained by centrifuging citrated human blood at 2500 rpm for 20 min and decanting the plasma into clean tubes for storage at −20 °C. The plasma samples were activated with 10 μL of 0.25% (v/v) pancreatic enzyme in the solution (100 μL of the received human plasma and 900 μL of H_2O containing 1 mM calcium ion).

Sequences of aptamers were as follows:

Aptamer-1: 5′-HS-$(CH_2)_6$-TTTTTTTTTTGGTTGGTGTGGTTG-G-3′

Aptamer-2: 5′-HS-$(CH_2)_6$-TTTTTTAGTCCGTGGTAGGGCAG-GTTGGGGTGACT-3′

FAM-labeled aptamer-2: 5′-FAM-$(CH_2)_6$-AGTCCGTGGTAGGG-CAGGTTGGGGTGACT-3′

Control random oligonucleotide: 5′-TAGCTATGGAATTCCTC-GTAGGCAACACA-3′

(19) Huang, C. C.; Yang, Z.; Lee, K. H.; Chang, H. T. *Angew. Chem., Int. Ed.* **2007**, *46*, 6824–6828.
(20) Chen, G.; Wang, Y.; Tan, L. H.; Yang, M. X.; Tan, L. S.; Chen, Y.; Chen, H. Y. *J. Am. Chem. Soc.* **2009**, *131*, 4218–4219.
(21) Xiang, M. H.; Xu, X.; Liu, F.; Li, N.; Li, K. A. *J. Phys.Chem. B* **2009**, *113*, 2734–2738.
(22) Taton, T. A.; Mirkin, C. A.; Letsinger, R. L. *Science* **2000**, *289*, 1757–1760.
(23) Liu, G. L.; Long, Y. T.; Choi, Y.; Kang, T.; Lee, L. P. *Nat. Methods* **2007**, *4*, 1015–1017.
(24) Cao, Y. C.; Jin, R.; Mirkin, C. A. *Science* **2002**, *297*, 1536–1540.
(25) Storhoff, J. J.; Lucas, A. D.; Garimella, V.; Bao, Y. P.; Muller, U. R. *Nat. Biotechnol.* **2004**, *22*, 883–887.
(26) Liu, X.; Dai, Q.; Austin, L.; Coutts, J.; Knowles, G.; Zou, J.; Chen, H.; Huo, Q. *J. Am. Chem. Soc.* **2008**, *130*, 2780–2782.
(27) Jin, R. C. *Angew. Chem., Int. Ed.* **2008**, *47*, 6750–6753.
(28) Xu, C. S.; Cang, H.; Montiel, D.; Yang, H. *J. Phys. Chem. C* **2007**, *111*, 32–35.
(29) Cang, H.; Xu, C. S.; Yang, H. *Chem. Phys. Lett.* **2008**, *457*, 285–291.
(30) He, H.; Ren, J. *Talanta* **2008**, *77*, 166–171.
(31) Shi, X. G.; Wang, S. H.; Meshinchi, S.; Van Antwerp, M. E.; Bi, X. D.; Lee, I. H.; Baker, J. R. *Small* **2007**, *3*, 1245–1252.
(32) Murphy, C. J.; Gole, A. M.; Stone, J. W.; Sisco, P. N.; Alkilany, A. M.; Goldsmith, E. C.; Baxter, S. C. *Acc. Chem. Res.* **2008**, *41*, 1721–1730.
(33) Jiang, W.; Kim, B. Y.; Rutka, J. T.; Chan, W. C. *Nat. Nanotechnol.* **2008**, *3*, 145–150.
(34) He, H.; Xie, C.; Ren, J. *Anal. Chem.* **2008**, *80*, 5951–5957.
(35) Li, J. L.; Wang, L.; Liu, X. Y.; Zhang, Z. P.; Guo, H. C.; Liu, W. M.; Tang, S. H. *Cancer Lett.* **2009**, *274*, 319–326.
(36) Elghanian, R.; Storhoff, J. J.; Mucic, R. C.; Letsinger, R. L.; Mirkin, C. A. *Science* **1997**, *277*, 1078–1081.
(37) Shen, Q. P.; Nie, Z.; Guo, M. L.; Zhong, C. J.; Lin, B.; Li, W.; Yao, S. Z. *Chem. Commun.* **2009**, *15*, 929–931.
(38) Liu, J. W.; Lu, Y. *J. Am. Chem. Soc.* **2004**, *126*, 12298–12305.
(39) Jiang, Y.; Zhao, H.; Zhu, N. N.; Lin, Y. Q.; Yu, P.; Mao, L. Q. *Angew. Chem., Int. Ed.* **2008**, *47*, 8601–8604.
(40) Jiang, T. T.; Liu, R. R.; Huang, X. F.; Feng, H. J.; Teo, W. L.; Xing, B. G. *Chem. Commun.* **2009**, *15*, 1972–1974.
(41) Liu, R.; Liew, R.; Zhou, J.; Xing, B. *Angew. Chem., Int. Ed.* **2008**, *47*, 3081–3081.
(42) He, W.; Huang, C. Z.; Li, Y. F.; Xie, J. P.; Yang, R. G.; Zhou, P. F.; Wang, J. *Anal. Chem.* **2008**, *80*, 8424–8430.
(43) Jiang, Z. L.; Liao, X. J.; Deng, A. P.; Liang, A. H.; Li, J. S.; Pan, H. C.; Li, J. F.; Wang, S. M.; Huang, Y. J. *Anal. Chem.* **2008**, *80*, 8681–8687.
(44) Mishra, A.; Ram, S.; Ghosh, G. *J. Phys. Chem. C* **2009**, *113*, 6976–6982.

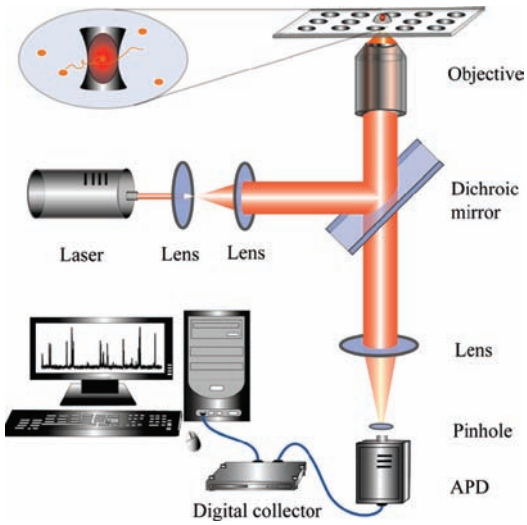

Figure 1. Schematic diagram of single gold nanoparticles counter (SGNPC). The setup was based on an inverted Olympus IX71 microscope. He−Ne laser with 632.8 nm was reflected by a dichroic mirror (650DRLP, Omega Optical, V), and then focused into a sample solution by a high numerical aperture water immersion objective (UplanApo, 60 × NA 1.2, Olympus, Japan). About 1−20 μL sample was placed on a coverslip. The scattering signal was collected after passing the 35 μm pinhole by an avalanche photodiode (SPCM-AQR14, Perkin-Elmer EG&G, Canada). The signal was recorded by a digital collector (Flex02-12D/C, Correlator.com, U.S.A.). The measurement time was 120 s, and the bin time was 1 ms.

Sequences of oligonucleotides in DNA hybridization were as follows:

Probe-1: 5′-HS-$(CH_2)_6$-$(A)_{10}$-AAGCTGCGTGATGAT-3′

Probe-2: 5′-GAAATCGGCTCCCGC-$(A)_{10}$-$(CH_2)_6$-SH-3′

Match target (A): 5′-GCGGGAGCCGATTTCATCATCACG-CAGCTT-3′

Single-base mismatch strand (B): 5′-GCGGGAGTCGATTTCAT-CATCACGCAGCTT-3′

Single-base mismatch strand (C): 5′-GCGGGAGACGATTTCAT-CATCACGCAGCTT-3′

Single-base mismatch strand (D): 5′-GCGGGAGGCGATTTCAT-CATCACGCAGCTT-3′

Instrumentations. The setup of SGNPC is shown in Figure 1, and is based on an inverted Olympus IX 71 microscope (Japan). He−Ne laser with 632.8 nm wavelength was reflected by a dichroic mirror (650DRLP, Omega Optical, U.S.A.), and then focused into the sample solution by a water immersion objective (UplanApo, 60 × NA1.2, Olympus, Japan). The sample was placed on a coverslip (thickness: 170 μm). The scattering signal was collected after passing the 35 μm pinhole by an avalanche photodiode (SPCM-AQR14, Perkin-Elmer EG&G, Canada). The signals obtained were recorded by a real time digital collector (Flex02-12D/C, Correlator.com, U.S.A.). The measurement time per sample was 120 s and the time interval was 1 ms. In the movie, images were obtained by an electron-multiplying charge-coupled device camera (EMCCD) camera with a frame-transfer device (Cascade 650, Photometrics). The frame transfer device has an imaging array of 653 × 492 with 7.4 × 7.4 μm^2/pixel.

Immunoassays of CEA and AFP. The procedure for synthesis of GNPs used in this study is provided in Supporting Information. Anti-CEA-1 functionalized GNPs conjugates (GNPs−anti-CEA-1) were prepared by adding 200 μL of 1 nM GNPs solution to 200 μL of 0.1 mg/mL anti-CEA-1 solution. The resultant mixture was allowed to react for 1 h at room temperature. The GNPs−anti-CEA-I conjugates were purified and washed by centrifugation two times at 2500 rpm for 30 min with the 0.01 M PBS buffer (containing 0.5 mg/mL BSA and 0.01 M phosphate buffer solution, pH 7.4) to remove excess antibodies. The pellet was redispersed in the 0.01 M PBS buffer and was stored at 4 °C for further use. The concentration of GNPs−anti-CEA-1 conjugates was determined using the SGNPC method described in this paper. The GNPs−anti-CEA-2, GNPs−anti-AFP-1 and GNPs−anti-AFP-2 conjugates were prepared by the same procedure described above.

Ten microliters of 0.25 nM GNPs−anti-CEA-1 conjugate solution, 10 μL of 0.25 nM GNPs−anti-CEA-2 conjugate solution and 20 μL of 0.01 M PBS buffer were added into a 200 μL sterilized polypropylene tube and mixed well. To each mixed solution, 10 μL of a solution of standard CEA antigen protein with different concentrations, or human sera, which were first 40 times diluted for normal human sera and 400 times diluted for cancer patient sera, were added and incubated at 37 °C for 1 h. Finally, the dilution of normal human sera was 200 times, and the dilution of cancer human sera was 2000 times with 0.01 M PBS buffer. The photon burst counts of sample solutions were measured by SGNPC. The measurement time per sample was 120 s, and the assay of each sample was repeated three times.

The immunoassays of AFP antigen in human serum samples were carried out according to the similar procedure above.

Assays of Thrombin. Thiol-labeled DNA−GNPs conjugates were prepared according to the protocols described by Mirkin and co-workers.[45,46] Twenty microliters of 100 μM aptamer-1 (or aptamer-2) was added to 1 mL of GNPs solution to obtain the final concentrations of 1 nM GNPs and 2.0 μM aptamer. After standing for 24 h, the solution was aged in 10 mM phosphate buffer (containing 0.1 M NaCl solution, pH 7.4) for 2 days. The aptamer−GNPs conjugates were washed by centrifugation (2500 rpm, 30 min) to remove excess reagents. The red pellet was washed with 0.1 M NaCl solution. After a second centrifugation, the pellet was brought to the original concentration in a 20 mM Tris solution (containing 0.5 mg/mL BSA, 140 mM NaCl and 10 mM KCl, pH 7.5). The concentration of aptamer−GNPs conjugates was determined using SGNPC method described in this paper.

Ten microliters of 0.3 nM GNPs−aptamer-1 conjugate solution, 10 μL of 0.3 nM GNPs−aptamer-2 conjugate solution and 20 μL 20 mM Tris solution (containing 0.5 mg/mL BSA, 140 mM NaCl and 10 mM KCl, pH 7.5) were added into a 200 μL sterilized polypropylene tube and mixed well. To each mixed solution, 10 μL standard solution of thrombin with different concentrations or activated human plasma sample solutions which were first diluted 2000 times were added, mixed well and incubated for 30 min at room temperature. Finally, the dilution of human plasma was 10,000 times. After incubation, about 20 μL sample solutions were subjected to a home-built SGNPC system. The measurement time per sample was 120 s, and the assay of each sample was repeated three times.

Assay of DNA Hybridization. GNPs−oligonucleotide conjugates were prepared according to the protocol described by Mirkin and co-workers.[45] Alkanethiol-capped oligonucletides were centrifuged at 14,000 rpm for 5 min. Oligonucletides were dissolved into 10 mM sodium phosphate buffer (pH 7). The final concentration of oligonucletides was 100 μM. Oligonucleotide-functionalized GNPs were prepared by incubation of 10 μL of 100 μM thiolated oligonucleotides (probe-1 or probe-2) in concentrated GNPs solution for 16 h at room temperature. This solution contained 650 pM GNPs and 5 μM oligonucleotides. Then, 40 μL of 10 mg/mL BSA was added to the mixture. The reaction mixture was then allowed to stand for 2 h. In the subsequent salt aging process, stepwise addition of NaCl up to 0.1 M was then made over another 24 h "aging" period, typically a three-step addition of salt at 8 h intervals. First, the functionalized GNPs solutions were brought to 0.1 M of NaCl by dropwise addition of 2 M NaCl solution and allowed to stand for 8 h, were then salted to 0.2 M of NaCl for standing 8 h, and finally were salted to 0.3 M NaCl and allowed to age for another

(45) Storhoff, J. J.; Elghanian, R.; Mucic, R. C.; Mirkin, C. A.; Letsinger, R. L. *J. Am. Chem. Soc.* **1998**, *120*, 1959–1964.
(46) Hirsch, L. R.; Jackson, J. B.; Lee, A.; Halas, N. J.; West, J. L. *Anal. Chem.* **2003**, *75*, 2377–2381.

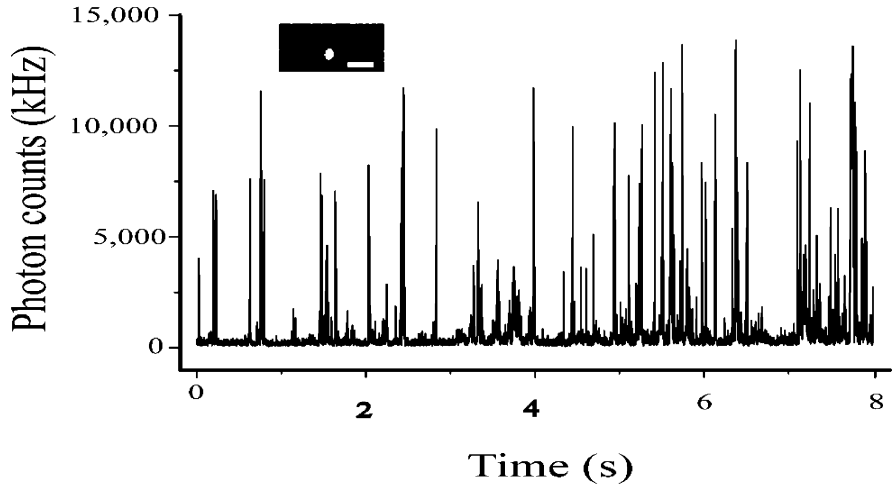

Figure 2. Typical photon burst trace of GNPs. (Inset) Image of single GNP in solution with 2 ms exposure time (without a pinhole); the scale bar is 2 μm. The GNPs size was 36.1 $\pm$ 4.0 nm, and the concentration was 0.17 nM.

8 h. Unbound oligonucleotides were subsequently removed by centrifugation (2500 rpm, 30 min). Following removal of the supernatant, the oily precipitate was then washed with 0.3 M PBS buffer (0.3 M NaCl, 0.125 mg/mL BSA and 10 mM phosphate buffer solution, pH 7), recentrifuged and redispersed in buffer. After washing two times, the functionalized GNPs solution was resuspended in buffer and stored at 4 °C for further use.

Twenty microliters of the as-prepared probe-1-functionalized GNPs and 20 μL of the as-prepared probe-2-functionalized GNPs in 0.3 M PBS buffer solution were added into a 200 μL sterilized polypropylene tube and mixed well. To each mixed solution, 10 μL of different concentrations of target DNA dissolved into 0.3 M PBS was added, and the mixtures were mixed well. DNA hybridization was performed on a Gene Amp PCR system 2400 (Applied Biosystems, U.S.A.). The hybridization protocol was similar to that in reference 47. The mixtures were first heated at 70 °C for 5 min and then quenched to 50 °C for 5 min. After the mixtures were cooled to room temperature, 20 μL of the sample solution was placed onto a cover slide and assayed by using our SGNPC. Each sample was measured five times, and the measurement time was 120 s.

Data Processing and Analyses. The photon burst traces of each sample were real time recorded by the data collector. The data files for each measurement were exported as hexadecimal ASCII files. The decimalized files could be calculated and plotted with Excel (Microsoft, WA) or Origin (OriginLab Corp., MA) software. Scattering light signals were integrated in 1 ms interval for a total measurement time of 120 s for each experiment. The photon burst counts could be obtained by the pick peak tool in Origin software using 3 times ratios of signal-to-noise. The calibration curve was obtained by plotting the photon burst counts against antigen, thrombin and oligonucleotide concentrations.

Results and Discussion

Principle and Design of SGNPC. Figure 1 shows schematics of SGNPC. The principle of SGNPC is based on the photon bursting of single GNPs in a small detection volume. When a single GNP diffuses into and out of the tiny illumination volume due to Brownian motion, the photon bursting can generate in this detection system, which can be real time monitored by an avalanche photodiode. The setup is similar to the fluorescence correlation spectroscopy (FCS) systerm,[48,49] except there is no emission filter. The tiny illumination volume is the key factor to get the high signal-to-noise ratio of single GNPs. Principally, the background scattering dramatically decreases and the scattering light of single GNPs basically remain constant with a decrease of the detection volume. Furthermore, the small detection volume can reduce the probability of simultaneously detecting multiple particles. In this setup, the confocal configuration and a high numerical aperture objective (NA 1.2) were used to dramatically reduce the detection volume, which efficiently limited the background scattering. The detection volume of SGNPC system was determined by FCS using Alexa 647 with the concentration of 1.0 nM (diffusion coefficient: 2.8 $\times$ 10^{-6} cm^2/s in water)[51] as standard substance. The detection volume obtained was about 0.9 fL.

Figure 2 shows a typical photon burst trace of 36 nm GNPs. The single bursts were mainly from single GNPs according to Poisson statistics as follows.[51,52]

$$P_m = \frac{\langle N \rangle^m}{m!} \exp(-\langle N \rangle) \quad (1)$$

Where m expresses the particle number, $\langle N \rangle$ is the average number of particles within the detection volume, and P_m is the probability that m particles occur in the detection volume.

On the basis of the formula (1), the P_m ($m = 1$) is calculated to be 8.4% for one particle and P_m ($m = 2$) to be 0.39% for two particles in the detection volume of 0.9 fL when the concentration of GNPs is 0.17 nM. This result demonstrated that the probability of simultaneously detecting two particles was very small.

As seen in Figure 2, the intensity of single bursts displayed dramatically differently. This difference was probably attributed to two aspects: the distribution of GNPs size and Gaussian profile of the focused laser beam. Transmission electron microscope (TEM) images of 36 nm GNPs showed the narrow distribution of GNP sizes, and thus the effects of the GNP size

(47) Xu, X.; Georganopoulou, D. G.; Hill, H. D.; Mirkin, C. A. *Anal. Chem.* **2007**, *79*, 6650–6654.
(48) Kim, S. A.; Heinze, K. G.; Schwille, P. *Nat. Methods* **2007**, *4*, 963–973.
(49) Dong, C.; Qian, H.; Fang, N.; Ren, J. *J Phys. Chem. B* **2006**, *110*, 11069–11075.
(50) Uyeda, H. T.; Medintz, I. L.; Jaiswal, J. K.; Simon, S. M.; Mattoussi, H. *J. Am. Chem. Soc.* **2005**, *127*, 3870–3878.
(51) Daniel, D. C.; Thompson, M.; Woodbury, N. W. *Biophys. J.* **2002**, *82*, 1654–1666.
(52) Földes-Papp, Z.; Demel, U.; Tilz, G. P. *J. Immunol. Meth.* **2002**, *260*, 117–124.

distribution should be insignificant in this case. Gaussian profile of the laser beam was a main factor affecting the intensity of single bursting. The laser intensity is strong in the center of the laser beam. When single GNPs passed far from the center of the laser beam, the photon bursting showed weaker; the intensive photon bursting occurred when single GNP passed to the center of the laser beam. Such strong photon bursting also can be monitored by a cooled electron-multiplying charge-coupled device camera (Supporting Information, video) and even by naked eyes. The inset of Figure 2 shows a typical image of a single GNP in solution obtained using a very short exposure time (2 ms) without a pinhole. The detection volume in this case was much larger than that with a pinhole. The dwell time of 36 nm GNPs was much longer than exposure time (2 ms).

The photon burst counts are associated with the detection volume, the diffusion coefficient and concentration of GNPs, the bin time and the measurement time. We approximately evaluated the photon burst counts of 36 nm GNPs to be 7200 in the detection volume of 0.9 fL when the concentration of GNPs was 0.17 nM and the measurement time was 120 s. The calculation is based on the diffusion coefficient of GNPs obtained from the Stokes−Einstein relation and the dwell time of GNPs provided by FCS. The detail of the calculation was given in Supporting Information. In this case, the measured result was about 2500 burst counts for 1 ms bin time, which were basically in agreement with the calculated result. The deviation between the measured and calculated results mainly originated from in the inaccurate concentration of GNPs and Gaussian profile of the focused laser beam. So far, we lack an efficient method for accurately characterization of GNPs concentration. In this study we calculated the GNPs concentration according to the size of GNPs measured by TEM imaging and the concentration of Au elements, which is a commonly used method. This measurement method led to the deviation from the "real" result. Due to Gaussian profile of the focused laser beam, the weak photon bursts of GNPs far away the center of the laser beam were not detected, which led to the decrease of the measured value. Additionally, in the calculation, we used the diameter of GNPs obtained by TEM instead of hydrodynamic diameter, which resulted in the increase of the calculated value.

The photon burst intensity markedly depended on the laser power and GNPs sizes. We investigated the effects of the laser illumination powers on the photon burst intensity of 36 nm GNPs using a 632.8 nm laser. We found that photon burst intensity increased with increase of illumination powers, and the results are shown in Figure S1 (Supporting Information). The signal overflow was observed under higher laser power (about 1 mW). The ratio of signal-to-noise is the highest at 0.10 mW. In order to study the effects of GNP sizes on the photon burst intensity, variable sizes of GNPs (55 nm, 36 nm, 25 and 17 nm) were prepared. The photon burst traces and TEM images of different GNPs are shown in Figure S2 (Supporting Information). These results show that the intensity of photon bursts increased dramatically with the diameters of GNPs. The signal overflow of 55 nm GNPs was observed at 0.10 mW illumination. Furthermore, we found that 55 nm GNPs (or bigger) was not very stable in solution as small GNPs (such as 36 nm) and the aggregation occurs in the storage process. Under optimal conditions, we compared the scattering intensity of GNPs (36 nm) with fluorescence intensity of quantum dots (QDs 655) and Alexa 647. The fluorescence was filtered by a band-pass filter (660DF50, Omega Optical, USA) in same detection system. As shown in Figure S3 (Supporting Information), the scattering light intensity of single GNPs was several tens to hundreds times higher than that of QDs and organic dyes.

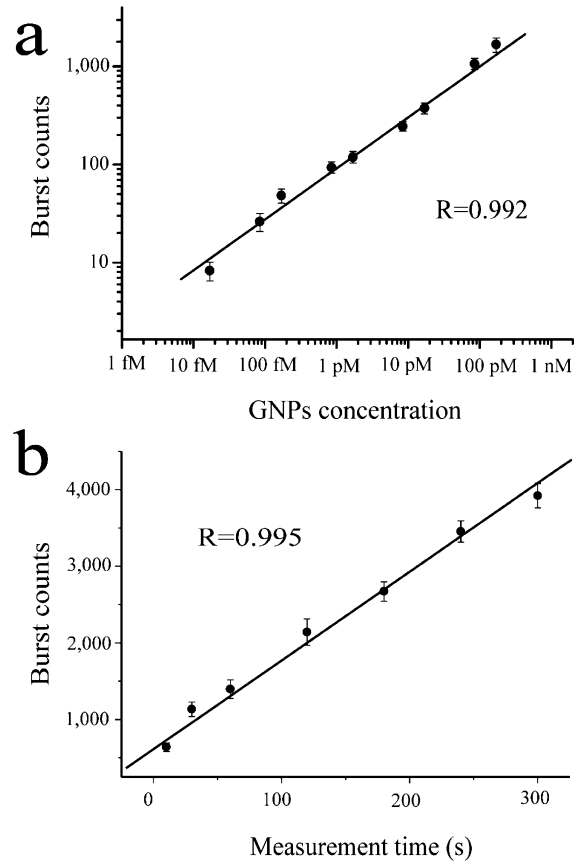

Figure 3. (a) Linear relationship between the photon burst counts and GNP concentrations. The GNP size was 36.1 ± 4.0 nm, the bin time was 1 ms and the measurement time was 120 s. (b) Linear relation between photon burst counts and the measurement time. The GNP size was 36.1 ± 4.0 nm, and the concentration was 0.17 nM, and the bin time was 1 ms. The error bars represent the standard deviation of 5 time measurements.

Figure 3a displays the excellent linear relationship between the photon burst counts and GNPs concentrations. The correlation coefficient (R) is 0.992, the linear range is over 4 orders of magnitude, and the detection limit is 17 fM GNPs (36 nm). In fact, the sensitivity of this assay can considerably enhance with the increasing of measurement time. Furthermore, we observed an excellent linear relationship between the photon burst counts and the measurement time (Figure 3b). This result documents that SGNPC may be used to real time monitor the certain chemical and biological processes using GNP as probes. We also investigated the effects of the bin time and the measurement time, and the results were shown in Supporting Information (Figure S4). We observed no distinguishable differences in the linearity and the slope of the calibration curves from 0.1 to 5 ms bin time, but the intensity of photon bursts were enhanced with an increase of the bin time. The relative standard deviations (RSDs) of photon burst counts decreased considerably with the increase of the measurement time. When the measurement time reached 120 s, the further increase of the measurement time had no significant improvement on the RSDs. When the bin time was 1 ms and the measurement time was 120 s, the reproducibility of the photon burst counting were quite satisfactory, and the RSDs for intraday and interday were 4.1% (n = 11) and 3.6% (n = 7), respectively. These results demonstrate

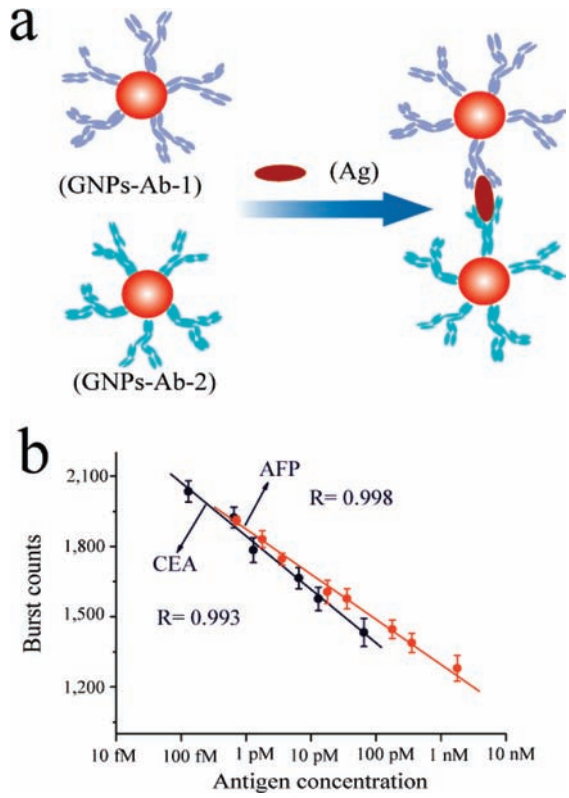

Figure 4. Principles of SGNPC-based homogeneous immunoassays. (a) Schematic illustration of homogeneous immunoassay. GNPs−Ab-1 and GNPs−Ab-2 represent two GNPs−antibody conjugates, respectively, and Ag represents antigen (CEA or AFP). (b) Linear relation between the burst counts and log CEA (AFP) concentration. The GNPs size was 36 nm. The concentrations of two GNPs-Ab conjugates were 60 pM. The bin time was 1 ms and the measurement time was 120 s. The error bars represent the standard deviation of five time measurements.

that SGNPC has ultrahigh sensitivity, high spatial (<1 fL) and good time resolutions, and good reproducibility.

Immunoassays of Cancer Biomarkers. In current clinical diagnosis, CEA and AFP are considered to be two very important biomarkers for liver cancer and certain cancers such as lung cancer, breast cancer and rectal cancer. It is reported that the AFP and CEA levels of cancer patient sera are significantly higher than those of healthy people. We used this technology to construct homogeneous immunoassays for AFP and CEA. Figure 4a displays the principle of a SGNPC-based homogeneous sandwich immunoassay. We conjugated two antibodies to GNPs (36 nm) based on the strong adsorption of GNPs to antibodies. The protocols for GNPs synthesis and bioconjugation were described in Supporting Information and Experimental Section. As shown in Figure 4a, when two GNPs−antibody conjugates are mixed in a sample containing antigens, the binding of antigens will cause GNPs to form dimers (or oligomers). We reasoned that the number of GNPs decreased with an increase of antigens in solution, and SGNPC sensitively detected the change in the number of GNPs according to the photon burst counts. The change in the photon burst counts of GNPs was mainly attributable to the decrease in particle number and the decreased diffusion coefficient due to the formation of larger particles such as dimers in the immune reaction. Figure 4b reflects good linear relations between the photon burst counts of GNPs and log CEA or log AFP concentration. The calibration curves of CEA and AFP have wide linear ranges over 3 orders of magnitude. The detection limits are 130 fM for CEA and 714 fM for AFP, respectively. Our methods are about 2 orders of magnitude more sensitive than current homogeneous methods.[9] The sensitivity of the assays was mainly dependent on binding constant, initial GNPs concentration and measurement time. As in conventional immunoassays, high binding constants also benefit for improvement of the sensitivity. The difference between the two assay sensitivities above should be attributed to different binding constants of antibodies raised against CEA and AFP. We observed that the increase of the measurement time decreased the deviation of the burst counting, which improved the reproducibility and the sensitivity. In theory, the low initial nanoparticle benefits for improvement of the sensitivity if the binding constants were high enough. However, we observed that GNPs−antibody concentrations had no significant effect on the assay sensitivity in the study concentration range (Supporting Information, Figure S5). This is probably due to the low concentration range of GNPs used in this study. We examined that the immunoassay reaction completed within 40 min (Supporting Information, Figure S6). The incubation time of 60 min was used in this study. The recoveries of the assays were higher than 90% (Supporting Information, Table S1). This method was successfully applied for direct determination of CEA and AFP levels in sera from healthy subjects and cancer patients. In measurements, human serum samples were 200−2000 times diluted with buffer, and the results are shown in Table 1. We observed that the CEA and AFP serum levels in cancer patients were much higher than those in healthy subjects. Our results were in good agreement with ELISA assays (Supporting Information). Notably, immunocomplexes were stable in solution, and the photon burst counts of GNPs remained constant for at least 4 h after the immune reaction. This result showed that the immunocomplexes probably existed as GNPs dimers or oligomers in the presence of the very low concentration of antigens.

Aptamer Recognition for Thrombin. Thrombin is a trypsin-like serine protease involved in a multitude of processes in the human body and can activate neutrophils and platelets which release cytokines, chemotactic factors and growth factors. Aptamers are nucleic acids that can bind specific protein sequences, similar to antibodies.[53] The aptamers for thrombin were prepared according to the refs 23, 43, and their sequences are shown in the Experimental Section. Figure 5a shows the principle of a thrombin assay using GNPs probes, which resembles a sandwich immunoassay. Thiol-capped aptamers were conveniently conjugated to GNPs via a Au−S bond. We observed a good linear relation between the photon burst counts of GNPs and log thrombin concentration (Figure 5b). The linear range is from 2.72 pM to 1.36 nM, and the detection limit is 2.72 pM. This sensitivity is 2 orders of magnitude higher than that of current methods.[45] The assay recovery was 94−107% (as shown in Table 2). This assay was applied for direct determination of thrombin in human plasma, and our results were in line with those obtained with the capillary electrophoresis assay (as shown in Table 2). The procedure and optimized conditions of the capillary electrophoresis assay were performed according to the protocol of refs 54−56 and are described in the Supporting Information. Under the optimized conditions, a

(53) Bock, L. C.; Griffin, L. C.; Latham, J. A.; Vermaas, E. H.; Toole, J. J. *Nature* **1992**, *355*, 564–566.
(54) Otsuka, H.; Akiyama, Y.; Nagasaki, Y.; Kataoka, K. *J. Am. Chem. Soc.* **2001**, *123*, 8226–8230.
(55) Zhang, H.; Li, X. F.; Le, X. C. *J. Am. Chem. Soc.* **2008**, *130*, 34–35.
(56) Li, Y.; Guo, L.; Zhang, F.; Zhang, Z.; Tang, J.; Xie, J. *Electrophoresis* **2008**, *29*, 2570–2577.

Table 1. CEA and AFP Levels in Serum Samples Measured by SGNPC and ELISA

	samples	CEA			AFP		
		SGNPC (M)	RSD (%)	ELISA (M)	SGNPC (M)	RSD (%)	ELISA (M)
1	normal	3.40×10^{-11}	6.8	4.56×10^{-11}	2.00×10^{-10}	4.7	1.47×10^{-10}
2	normal	3.66×10^{-11}	6.8	3.25×10^{-11}	2.36×10^{-10}	8.7	2.13×10^{-10}
3	normal	2.08×10^{-11}	8.8	1.92×10^{-11}	3.41×10^{-10}	10.3	2.90×10^{-10}
4	normal	3.69×10^{-11}	10.7	2.81×10^{-11}	2.09×10^{-10}	6.5	1.91×10^{-10}
5	normal	1.56×10^{-11}	3.6	3.27×10^{-11}	4.09×10^{-10}	10.4	3.21×10^{-10}
6	pregnant	3.01×10^{-11}	5.4	4.55×10^{-11}	5.47×10^{-10}	8.0	4.73×10^{-10}
7	lung cancer	1.20×10^{-8}	6.1	1.48×10^{-8}	2.48×10^{-10}	6.4	2.39×10^{-10}
8	rectal cancer	9.04×10^{-9}	5.1	8.59×10^{-9}	4.04×10^{-10}	7.1	3.09×10^{-10}
9	liver cancer	5.64×10^{-10}	3.9	4.72×10^{-10}	1.36×10^{-9}	9.6	1.91×10^{-9}

satisfactory separation result and quantitative relationship were obtained, which are shown in the Supporting Information (Figure S6).

DNA Hybridization Detection. Another key application of SGNPC is homogeneous DNA hybridization detection. The DNA hybridization principle using GNPs probes is shown in Figure 6a, which resembles the reported sandwich strategy.[23] In this study we chose a fragment of methylenetetrahydrofolate reductase (MTHFR) gene as a target. MTHFR gene has a common polymorphism 677C → T, which may result in low serum folate and hyperhomocysteinemia.[57,58] The sequences of two probes, complete match containing 677 site and mismatch target DNA fragments were shown in the Experimental Section. We linked two thiol-capped oligonucleotides to GNPs via a Au−S bond. The protocols for linkage of GNPs with oligonucleotides are described in the Experimental Section. Figure 6b shows good linear relations between the photon burst counts of GNPs and log target concentration under different conditions. The change in the concentration of GNPs−oligonucleotide conjugates had no significant effect on the detection sensitivity of DNA target (the slop of calibration curve) in the study concentration range. However, with the increase of GNPs−oligonucleotide conjugates concentration, the linear range became wider and the correlation became better, but the sensitivity became sightly decreased. The linear ranges are close to 2 orders of magnitude (lines 2 and 3), and the detection limits are 0.5 fM, 1 fM and 4 fM, respectively. This sensitivity is equivalent to about 10^3 copies/μL DNA level, which is about 2−5 orders of magnitude higher than that obtained with current methods.[22−25,58,59] Such high sensitivity is due to use of SGNPC technique and DNA-modified GNPs probes. It is reported that DNA heavily modified GNPs probes exhibit high target binding constants, which increase the assay sensitivity.[22,25] The hybridization products were stable in solution, and the photon burst counts of GNPs remained constant for at least 5 h after hybridization.

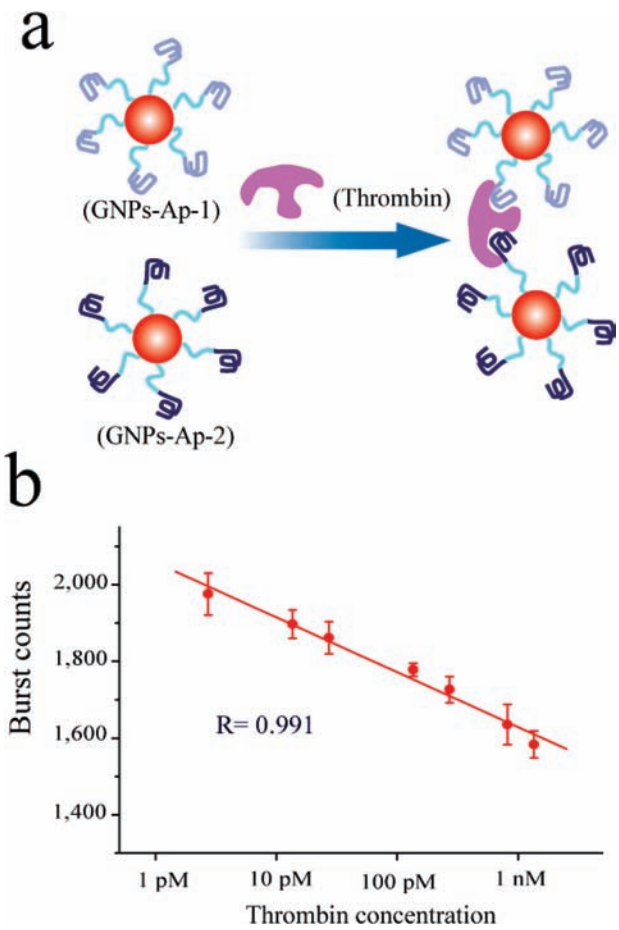

Figure 5. Principles of SGNPC-based aptamer recognition for thrombin. (a) Schematic illustration of affinity reaction between aptamer-based probes and thrombin. GNPs−Ap-1 and GNPs−Ap-2 represent two GNPs−aptamer conjugates, respectively. (b). Linear relation between the burst counts and log thrombin concentration. The concentrations of two GNPs−aptamer conjugates were 60 pM. The buffer was 20 mM Tris solution (containing 0.5 mg/mL BSA, 140 mM NaCl and 10 mM KCl, pH 7.4). The bin time was 1 ms and the measurement time was 120 s. The error bars represent the standard deviation of five time measurements.

We also tested this assay selectivity. Different single base mismatch DNA fragments (G/T, G/A and G/G) were used as targets in hybridization. The results are shown in Figure 6c. We observed that the burst count changes of single base mismatch DNA fragments were much lower than those of the match target. Our preliminary results demonstrated that this assay unambiguously distinguished DNA sequences with single base mismatches.

Conclusion

In this paper, we first proposed the SGNPC assay design, and then we developed an ultrasensitive and highly selective detection platform for homogeneous immunoassay and DNA hybridization at femtomolar level based on SGNPC techniques. Our method was successfully used to directly detect cancer biomarkers from clinical samples. Compared to current methods, our method can be characterized as extremely high sensitivity, good selectivity, simplicity and short analysis time. More

(57) Frosst, P.; Blom, H. J.; Milos, R.; Goyette, P.; Sheppard, C. A.; Matthews, R. G.; Boers, G. J. H.; Den Heijer, M.; Kluijtmans, L. A. J.; Van den Heuvel, L. P.; Rozen, R. *Nat. Genet.* **1995**, *10*, 111–113.
(58) Jenison, R.; Yang, S.; Haeberli, A.; Polisky, B. *Nat. Biotechnol.* **2001**, *19*, 62–65.
(59) Reynolds, R. A.; Mirkin, C. A.; Letsinger, R. L. *J. Am. Chem. Soc.* **2000**, *122*, 3795–3796.

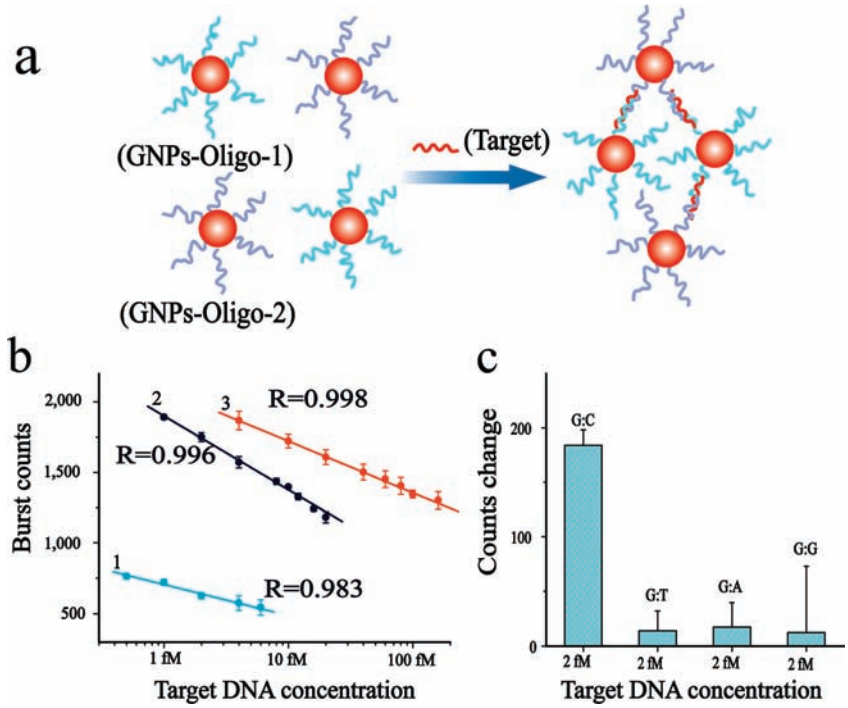

Figure 6. Principles of SGNPC-based DNA hybridization. (a) Schematic illustration of DNA hybridization. GNPs−Oligo-1 and GNPs−Oligo-2 represent two GNPs−oligonucleotide conjugates, respectively. (b) Log−linear relationship between the burst counts and the match target concentration in different concentrations of GNPs−oligonucleotide solutions (1: 30 pM, 2: 60 pM, 3: 100 pM). (c) The histograms of the burst counts change from the complete match (G/C) and three single base mismatch DNA fragments (G/T, G/A and G/G) as targets in hybridization. The count changes stand for the burst count differences without and with targets. The target concentrations were 2 fM. The bin time was 1 ms, and the measurement time was 120 s. The error bars represent the standard deviation of five time measurements.

Table 2. Thrombin Assay in Plasma

	SGNPC					
	thrombin (M)	RSD (%)	added (M)	found (M)	recovery (%)	CE-LIF thrombin (M)
plasma 1	5.49×10^{-7}	6.8	5.45×10^{-11}	1.06×10^{-10}	93.9	4.65×10^{-7}
plasma 2	6.08×10^{-7}	5.1	5.45×10^{-11}	1.18×10^{-10}	105.0	5.67×10^{-7}
plasma 3	5.44×10^{-7}	6.3	5.45×10^{-11}	1.11×10^{-10}	106.7	4.49×10^{-7}
plasma 4	5.29×10^{-7}	6.1	5.45×10^{-11}	1.09×10^{-10}	102.2	4.41×10^{-7}

In recovery experiments, a given amount of thrombin was added into the plasma after the sample was 10,000 times diluted with buffer. The samples were then measured by SGNPC. The RSD was derived from three independent experiments.

importantly, our detection volume is less than 1 fL, and the sample requirement can easily be reduced to nanoliter level using a droplets array.[60,61] Therefore, our method has the potential to become a high- throughput detection platform for homogeneous immunoassay and DNA (RNA) assays similar to currently used microarray biochips. The assay sensitivity allows detection of several tens of copies of DNA or RNA when the sample volume is about 10 nL using droplets arrays. Thus, our method can be used to directly determine mRNA and micro-RNA levels and even genomic DNA in cells, viruses, bacteria and tissues without PCR and signal amplifications. Furthermore, SGNPC can be used for real-time monitoring of certain biochemical processes in vitro and vivo due to its high spatial and good time resolutions.

Acknowledgment. This work was financially supported by NSFC (20675052, 20727005, 20705019), National High-Tech Research and Development Program (2006AA03Z324) and National Basic Research Program of China (2009CB930400). J.C.R. thanks Prof. Daode Hu (Shanghai Jiaotong University Affiliated Shanghai First People's Hospital) for providing cancer patient sera.

Supporting Information Available: Supporting methods; typical photon burst traces of GNPs solution; photon burst traces of different size GNPs and their transmission electron microscope image; comparison of the photon burst traces of GNPs, quantum dots and Alexa 647; linear relationship of the burst counts and GNP concentration; titration curves of alpha fetal protein (AFP) with different antibody−GNPs conjugate concentrations; curve of burst counts versus immunoassay reaction time; results of thrombin assay by capillary electrophoresis; recovery results of CEA and AFP immunoassays; movie of GNPs photon bursts in solution; and complete ref 1. This material is available free of charge via the Internet at http://pubs.acs.org.

(60) Song, H.; Chen, D. L.; Ismagilov, R. F. *Angew. Chem., Int. Ed.* **2006**, *45*, 7336–7356.
(61) Shi, W.; Qin, J.; Ye, N.; Lin, B. *Lab Chip* **2008**, *8*, 1432–1435.

JA903873N